Hindawi
Complexity
Volume 2020, Article ID 3062859, 10 pages
https://doi.org/10.1155/2020/3062859

Research Article

Statistical Characteristics of the First Passage Time Analysis for the Gene Regulatory Circuit in *Bacillus subtilis* by Cell Mapping Method

Liang Wang,[1] Minjuan Yuan ,[1] Shichao Ma,[2] Xiaole Yue,[1] and Ying Zhang [1]

[1]*Department of Applied Mathematics, Northwestern Polytechnical University, Xi'an 710129, China*
[2]*School of Astronautics, Northwestern Polytechnical University, Xi'an 710072, China*

Correspondence should be addressed to Minjuan Yuan; minjuanyuan@mail.nwpu.edu.cn

Received 15 October 2019; Revised 23 December 2019; Accepted 8 January 2020; Published 5 February 2020

Academic Editor: Alejandro F. Villaverde

Copyright © 2020 Liang Wang et al. This is an open access article distributed under the Creative Commons Attribution License, which permits unrestricted use, distribution, and reproduction in any medium, provided the original work is properly cited.

In this paper, we will explore the stochastic exit problem for the gene regulatory circuit in *B. subtilis* affected by colored noise. The stochastic exit problem studies the state transition in *B. subtilis* (from competent state to vegetative state in this case) through three different quantities: the probability density function of the first passage time, the mean of first passage time, and the reliability function. To satisfy the Markov nature, we convert the colored noise system into the equivalent white noise system. Then, the stochastic generalized cell mapping method can be used to explore the stochastic exit problem. The results indicate that the intensity of noise and system parameters have the effect on the transition from competent to vegetative state in *B. subtilis*. In addition, the effectiveness of the stochastic generalized cell mapping method is verified by Monte Carlo simulation.

1. Introduction

B. subtilis, which is a single-celled creature, is simpler and easier than multicellular creature [1]. It includes three physiological states: vegetative state, competent state, and sporulation. When there is sufficient nutrition, *B. subtilis* is in vegetative state and performs normal life activities. In the case of nutrient limitation, a minority of *B. subtilis* cells become competent state, while most of them form sporulation. Sporulation is a dormant body rather than a propagule. Once sporulation forms, *B. subtilis* maintains this state until the environment improves [2]. The competent cell can switch to vegetative state with a certain probability. The state transition can be attributed to the excitability in the gene regulatory circuit.

Cells can use the gene regulatory circuit to implement the state transition [3]. This process is affected by the fluctuations [4], which arise from processes intrinsic or extrinsic to gene expression [5]. Kohar and Lu studied the effect of both the intrinsic and extrinsic noises and parameters on the dynamics of gene regulatory circuits through the randomization-based approach [6]. Intrinsic noise results from stochasticity in the biochemical reactions at an individual gene. In 2010, Dandach and Khammash had presented a novel numerical method for the analysis of stochastic biochemical events and then studied the genetic circuit regulating competence under the excitation of intrinsic noise in *B. subtilis* [7]. Extrinsic noise is the additional variation originating from the fluctuation in the cellular components and has a global effect on the dynamics of the system. In addition, the Ornstein–Uhlenbeck noise (the colored noise), which is a time-correlated noise with zero mean [8], is closer to the actual cell behavior [2]. Thus, we mainly consider the extrinsic colored noise in *B. subtilis* in this paper.

To confirm the state of *B. subtilis*, it is necessary to understand ComK gene. The ComK gene, a regulatory transcription unit, is essential for the development of genetic competence in *B. subtilis* [9]. When the concentration of ComK protein is high, *B. subtilis* is in the competent state.

Conversely, when the concentration of ComK protein is low, *B. subtilis* is in the vegetative state. Therefore, we can judge which state *B. subtilis* is in by analyzing the concentration of ComK protein.

The stochastic exit problem is usually used to analyze such state transition through three quantities: the probability density function of first passage time (PDF of FPT), the mean of first passage time (MFPT), and the reliability function [10, 11]. FPT refers to the time that it takes for a trajectory in the system to start from a stable equilibrium point and then cross the boundary of security region and reach the target region for the first time. Broadly stated, the FPT refers to the time that *B. subtilis* takes to finish the transition from the stable competent state to stable vegetative state in this paper. In this context, the PDF of FPT refers to the probability that *B. subtilis* finishes the transition as time goes on. Mathematically, the MFPT is the expectation of the FPT. Concretely, the MFPT refers to the mean time that *B. subtilis* needs to achieve the state transition. The reliability function indicates the change relation between the reliability of system and time, which represents the probability that *B. subtilis* remains in the competent state as time goes on. In the paper, we study the stochastic exit problem for the gene regulatory circuit in *B. subtilis* with colored noise through the above three different quantities.

The cell mapping method [12], which is an efficient numerical method to analyze global dynamics, was firstly suggested by Hsu in 1980. Later, many scholars have developed new versions. Among them, the composite cell coordinate system (CCCS) method [13, 14] is usually used to obtain the global properties in the deterministic system, containing attractor, basin of attraction, boundary, and so on. The stochastic generalized cell mapping (SGCM) method [15, 16] is used to obtain the stochastic response [17–19] in the stochastic system.

The rest of this paper is as follows. In Section 2, we give the deterministic model of gene regulatory circuit in *B. subtilis* and then determine the security domain and boundary. The effect of noise on the PDF of FPT, MFPT, and reliability function in the stochastic system are shown in Section 3. We research the effect of system parameters on the three quantities in the stochastic system in Section 4. In Section 5, the conclusions are presented.

2. Model Introduction and the Determination of Security Domain

An excitable core module contains positive and negative feedback loops [2], which were found by Süel et al. in 2006. The module can explain the mechanism of entering or exiting the competent state very well [20, 21]. Both the positive and negative feedback loops consist of four important parts: First, the ComK activates itself via a transcriptional autoregulatory positive feedback loop, which results in the basal expression of ComK and the beginning of this core module. Thus, the ComK transcription factor is the heart of this circuit. Second, the ComK proteins can be degraded by MecA via enzymatic degradation. Third, the degradation of ComK is inhibited by the ComS, because ComS can also bind with MecA competitively. Fourth, the overexpression of ComK inhibits the synthesis of ComS. The enzymatic degradation reactions are assumed to be of the standard Michaelis–Menten form [2]:

$$\begin{aligned} &\mathrm{MecA} + \mathrm{ComK} \overset{\gamma_{\pm a}}{\rightleftharpoons} \mathrm{MecA-ComK} \xrightarrow{\gamma_1} \mathrm{MecA}, \\ &\mathrm{MecA} + \mathrm{ComS} \overset{\gamma_{\pm b}}{\rightleftharpoons} \mathrm{MecA-ComS} \longrightarrow^{\gamma_2} \mathrm{MecA}. \end{aligned} \tag{1}$$

In the following, the symbols K and S represent the concentrations of ComK protein and ComS protein, respectively. The concentrations of free MecA and the complexes MecA-ComK and MecA-ComS can be denoted by M_f, M_K, and M_S, respectively. Meanwhile, the total amount of M_f, M_K, and M_S is determined in an enclosed living environment of *B. subtilis*. Hence, the relationship among free MecA, complexes MecA-ComK, and complexes MecA-ComS can be expressed [2, 22] by

$$M_f + M_K + M_S = M_{\text{total}} = \text{constant}. \tag{2}$$

The following equations describe the relationship among K, S, and MecA [7]. Other symbols are the system parameters, whose description are given in Table 1 [2]:

$$\begin{aligned} \frac{\mathrm{d}K}{\mathrm{d}t} &= \alpha_k + \frac{\beta_k K^n}{k_k^n + K^n} - \gamma_a M_f K + \gamma_{-a} M_K, \\ \frac{\mathrm{d}S}{\mathrm{d}t} &= \frac{\beta_s}{1 + (K/k_s)^p} - \gamma_b M_f K + \gamma_{-b} M_S, \\ \frac{\mathrm{d}M_K}{\mathrm{d}t} &= -(\gamma_{-a} + \gamma_1) M_K + \gamma_a M_f K, \\ \frac{\mathrm{d}M_S}{\mathrm{d}t} &= -(\gamma_{-b} + \gamma_2) M_K + \gamma_b M_f S. \end{aligned} \tag{3}$$

Through dimensionless, the final simplified equations [2] are as follows:

$$\begin{aligned} \frac{\mathrm{d}K}{\mathrm{d}t} &= a_k + \frac{b_k K^n}{k_0^n + K^n} - \frac{K}{1 + K + S}, \\ \frac{\mathrm{d}S}{\mathrm{d}t} &= \frac{b_s}{1 + (K/k_1)^p} - \frac{S}{1 + K + S}. \end{aligned} \tag{4}$$

Here, $a_k = \alpha_k/(\delta_k \Gamma_k)$, $b_k = \beta_k/(\delta_k \Gamma_k)$. $b_s = \beta_s/(\delta_s \Gamma_s)$, $k_0 = k_k/\Gamma_k$, $k_1 = k_s/\Gamma_k$, $\Gamma_k = (\gamma_{-a} + \gamma_1)/\gamma_a$, $\Gamma_s = (\gamma_{-b} + \gamma_2)/\gamma_b$, $\delta_k = (\gamma_1 M_{\text{total}})/\Gamma_k$, and $\delta_s = (\gamma_2 M_{\text{total}})/\Gamma_s$.

The primary task is to obtain the global properties through the CCCS method, which includes attractor, basin of attraction, and boundary. Thus, the security domain, target domain, and boundary can be determined. The attractor, which represents the steady response of the dynamical system, corresponds to the stable state of *B. subtilis*. The basin of attraction indicates the region which is either security or target region. The security region and the target region are divided by the boundary. In the following, $\Omega = \{(K, S) \mid 0 \le K \le 0.6, 0 \le S \le 10\}$ is selected the interesting domain, and the parameters are taken [2] as $a_k = 0.004$, $k_0 = 0.2$, $k_1 = 0.222$, $n = 2$, and $p = 5$.

Table 1: Description of parameters in the dynamical model.

Parameter	Description
α_k	Basal expression rate of ComK
β_k	Saturating expression rate of ComK positive feedback
β_s	Unrepressed expression rate of ComS
k_k	ComK concentration for half-maximal ComK activation
k_s	ComK concentration for half-maximal ComS repression
δ_k	Unrepressed degradation rate of ComK
δ_s	Unrepressed degradation rate of ComS
Γ_k	ComK concentration for half-maximal degradation
Γ_s	ComS concentration for half-maximal degradation
n	Hill coefficient of ComK positive feedback
p	Hill coefficient of ComS repression by ComS

Without loss of generality, this work is focused on the transition from competent to vegetative state in *B. subtilis*. As shown in Figure 1, the blue triangle A1 represents attractor, which means the stable vegetative state of *B. subtilis*. Similarly, the red diamond A2 is another attractor that denotes the stable competent state. The cyan region B1 and yellow region B2 represent the basin of attraction of attractors A1 and A2, respectively. The two basins of attraction are divided by the boundary shown by the dark green curve. In this paper, we choose attractor A2 as the start point. The yellow region B2 is the security domain, while the cyan region B1 represents the target region. Hence, the FPT refers to the time it takes for the trajectory to start from A2, then cross the boundary (the dark green curve), and reach B1 for the first time. The PDF of FPT represents the possibility that the trajectory crosses the boundary for the first time as time goes on. The MFPT refers to the average time that the trajectory takes to cross the boundary for the first time. The reliability function refers to the possibility that the trajectory remains in the security region B2 over time.

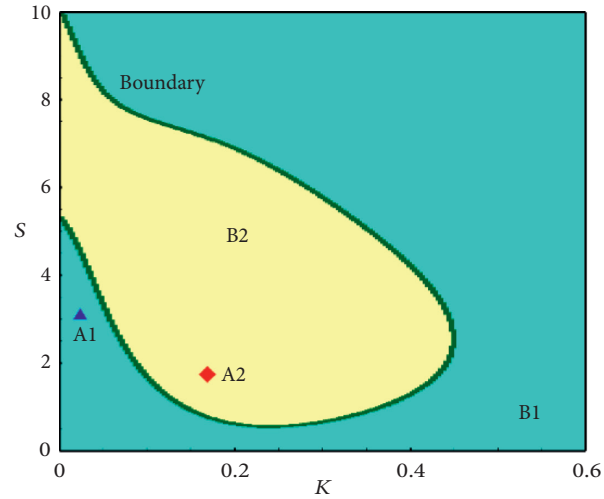

Figure 1: The global dynamic character of system (4): $b_k = 0.13$; $b_s = 0.75$.

3. Effect of Noise on the FPT Statistics and Reliability of System

In fact, an excitable system is sensitive to noise. According to the experimental results [4], the colored noise [8] may be more compatible with actual fluctuations than the white noise (4). The gene regulatory circuit in *B. subtilis* affected by colored noise is as follows [2]:

$$\begin{aligned} \frac{\mathrm{d}K}{\mathrm{d}t} &= a_k + \frac{b_k K^n}{k_0^n + K^n} - \frac{K}{1+K+S}, \\ \frac{\mathrm{d}S}{\mathrm{d}t} &= \frac{b_s}{1+(k_1/k_1)^p} - \frac{S}{1+K+S} + \xi(t). \end{aligned} \tag{5}$$

Here, $\xi(t)$ is the Ornstein–Uhlenbeck noise and the properties of $\xi(t)$ can be written as $\langle \xi(t) \rangle = 0$ and $\langle \xi(t)\xi(t') \rangle = D\lambda \exp(-\lambda|t-t'|)$, where D is the noise strength and λ is the inverse of the correlation time τ_c.

Then, the SGCM method will be used to compute the PDF of FPT, MFPT, and reliability function of system (5). The Markov nature should be satisfied before the SGCM method is used. However, the colored noise obviously does not satisfy this nature. In order to resolve this contradiction, we convert the stochastic dynamical system with the colored noise into the equivalent one with white noise [8], which satisfies the Markov nature well. The equivalent stochastic dynamical system is as follows:

$$\begin{aligned} \frac{\mathrm{d}K}{\mathrm{d}t} &= a_k + \frac{b_k K^n}{k_0^n + K^n} - \frac{K}{1+K+S}, \\ \frac{\mathrm{d}S}{\mathrm{d}t} &= \frac{b_s}{1+(K/k_1)^p} - \frac{S}{1+K+S} + \eta, \\ \frac{\mathrm{d}\eta}{\mathrm{d}t} &= h(\eta) + \lambda g_w(t). \end{aligned} \tag{6}$$

Here, $h(\eta) = -\lambda\eta$ and g_w is the Gaussian white noise with properties $\langle g_w(t) \rangle = 0$ and $\langle g_w(t) g_w(t') \rangle = 2D\delta(t-t')$. Moreover, $\eta(t)$ satisfies $\langle \eta(t) \rangle = 0$ and $\langle \eta(t)\eta(t') \rangle = D\lambda \exp(-\lambda|t-t'|)$, and the initial distribution is $P(\eta_0) = (2\pi D\lambda)^{-1/2} \exp(-\eta_0^2/2D)$.

In this part, we will study the effect of noise on the PDF of FPT, MFPT, and reliability function of system (6). More concretely, we analyze how the noise strength D and the inverse of the correlation time λ affect the three

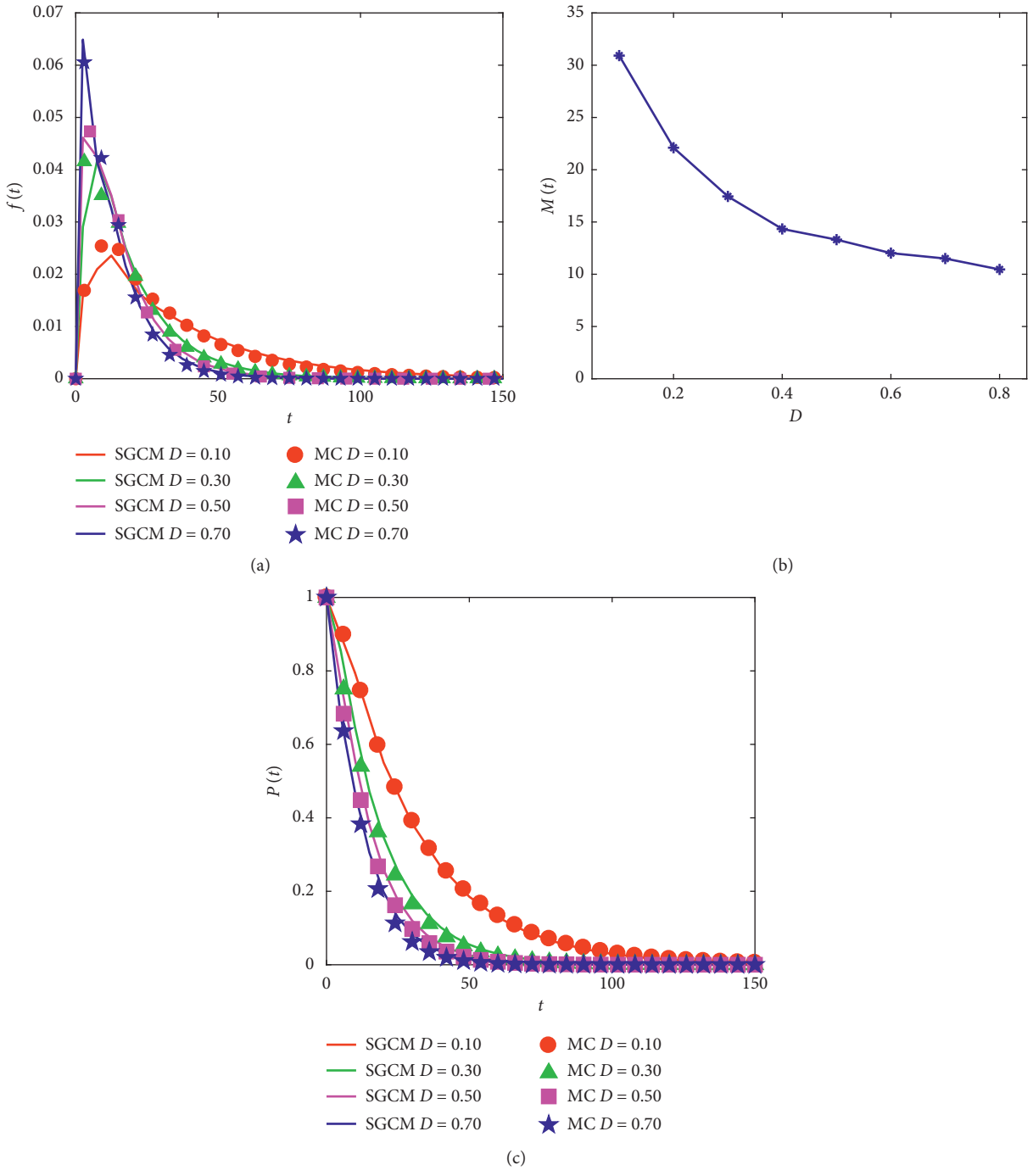

FIGURE 2: (a) PDF of FPT of system (6): $\lambda = 0.30$. (b). MFPT of system (6): $\lambda = 0.30$. (c) Reliability function of system (6): $\lambda = 0.30$.

quantities through the SGCM method. The stable competent state A2, the security domain B2, the target region B1, and boundary are shown in Figure 1. Note that the symbols $f(t)$, $M(t)$, and $P(t)$, respectively denote the PDF of FPT, MFPT, and reliability function in the following figures.

The PDF of FPT is shown in Figure 2(a) with $b_k = 0.13$, $b_s = 0.75$, and $\lambda = 0.30$. For $f(t)$ with different noise strength D, there is the same trend, i.e., as the time t increases, all $f(t)$ increases from initial value $f(0) = 0$ to the peak value, then gradually decreases, and finally returns to 0. The difference is the peak of $f(t)$. As the noise strength D increases from 0.10 to 0.70, the peak of $f(t)$ gradually increases, the time corresponding to the peak reduces and the time that $f(t)$ takes to drop from the peak to zero also becomes short. These results show that probability that *B. subtilis* achieves the state transition becomes large as D increases. As shown in Figure 2(b), we can find that $M(t)$ reduces from 31 to 10 as D varies from 0.10 to 0.80. Moreover, the corresponding reliability function is shown in Figure 2(c). As the noise strength D increases, the

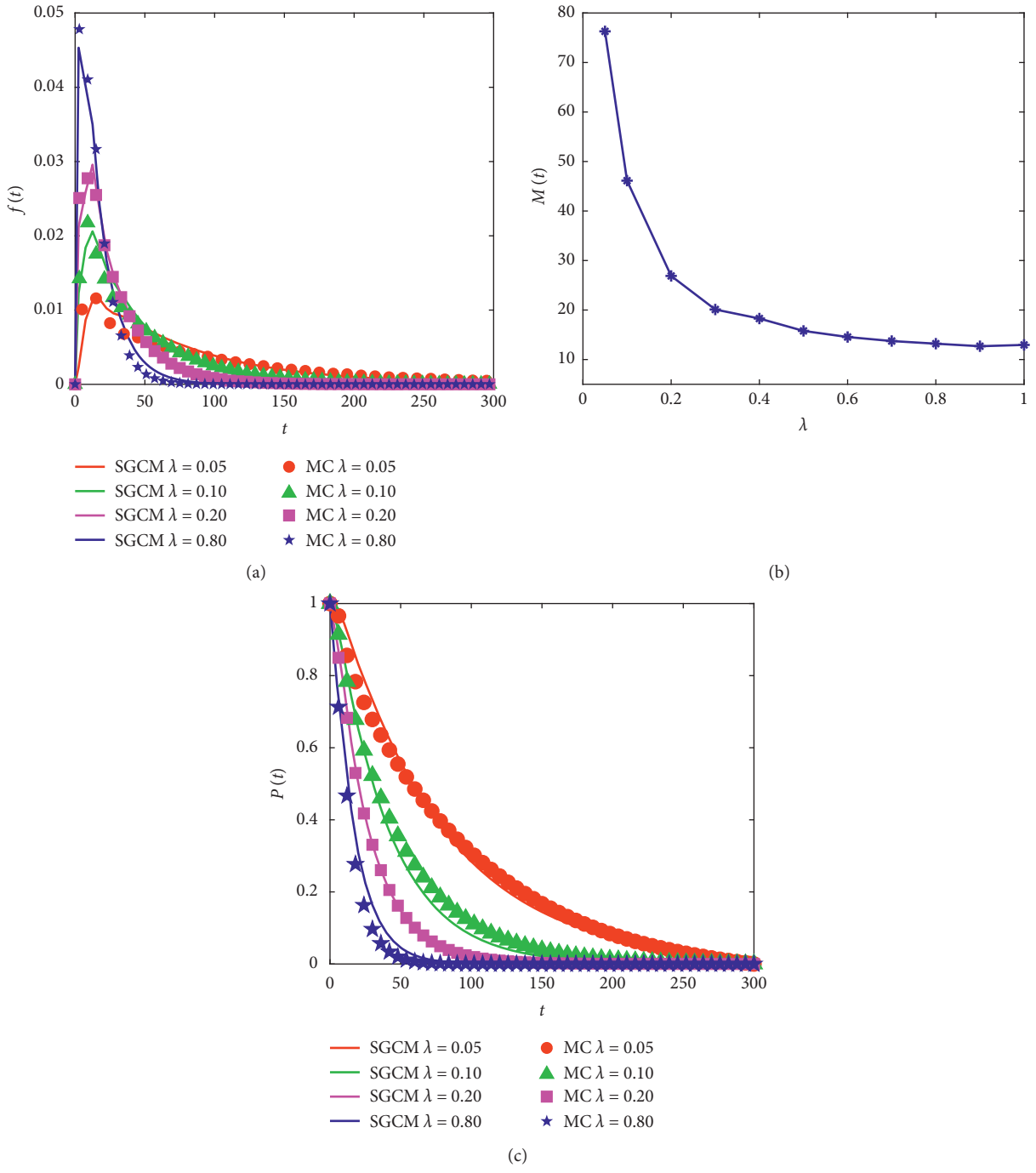

FIGURE 3: (a) Probability density function of FPT of system (6): $D = 0.20$. (b) MFPT of system (6): $D = 0.20$. (c) Reliability function of system (6): $D = 0.20$.

curve becomes steep, which indicates the reliability of the system is weakened. These above results indicate that as D increases, it becomes easy for the trajectory to pass through the boundary and reach the target region B1. That is, the transition (from competent to vegetative state) in *B. subtilis* becomes easy. Therefore, we can conclude that the larger the noise strength D, the easier the state transition in *B. subtilis*. In addition, the results obtained by the SGCM method agree well with the Monte Carlo (MC) simulation method, which shows the effectiveness of the SGCM method.

The effect of λ on $f(t)$, $M(t)$, and $P(t)$ is shown in Figure 3 with $b_k = 0.13$, $b_s = 0.75$, and $D = 0.20$. In Figure 3(a), it can be found that the value of $f(t)$ increases firstly and then gradually decreases. Obviously, as λ increases, the time that $f(t)$ takes to drop from the peak to zero becomes short, while the time corresponding to the peak is about the same, which shows probability that *B. subtilis* achieves the transition from the competent to vegetative state becomes large as λ increases. As shown in Figure 3(b), we can find that $M(t)$ reduces from 76 to 12 as

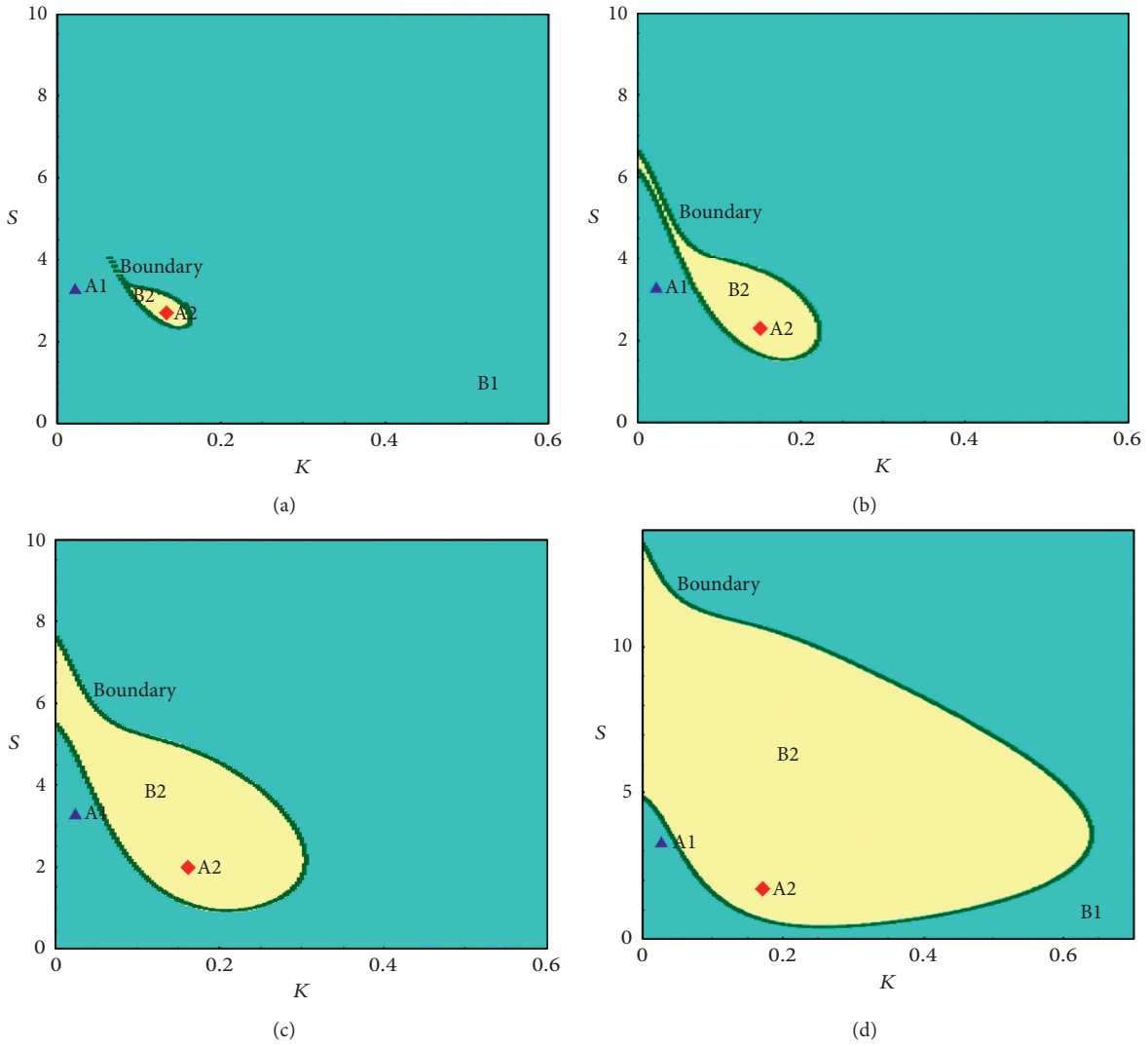

Figure 4: The global dynamic character of system (4): $b_s = 0.76$ (a) $b_k = 0.10$, (b) $b_k = 0.11$, (c) $b_k = 0.12$, and (d) $b_k = 0.13$.

λ varies from 0.05 to 1.00. The corresponding reliability function $P(t)$ is shown in Figure 3(c). The curvature of curve increases with the increase of λ, which indicates the reliability of the system is weakened. These results indicate that it becomes easy for a trajectory to pass through the boundary and reach the target region B1. And the reliability of the system is weakened with the increase of λ, which means the transition (from competent to vegetative state) in *B. subtilis* becomes easy. In other words, the larger the inverse of the correlation time, the easier the state transition in *B. subtilis*. Similarly, the results obtained by the SGCM method are in accordance with the MC simulation.

4. Effect of System Parameters on the FPT Statistics and Reliability of System

In this section, we analyze how the system parameters b_k and b_s affect the PDF of FPT, MFPT, and reliability function of system (5). The noise parameters are taken as $D = 0.20$ and $\lambda = 0.20$ in the following.

The effect of parameter b_k is discussed firstly. Figure 4 shows clearly the global properties of system (5) for different b_k. It is obvious that the area of security domain B2 becomes large with the increase of b_k, while the area of the target region B1 becomes small. In theory, the phenomenon indicates that the state transition (from competent to vegetative state) becomes difficult.

Figure 5(a) presents the change of the PDF of FPT as b_k varies. We can see that $f(t)$ still has only one peak. As b_k increases from 0.10 to 0.13, the peak of $f(t)$ reduces and the time that $f(t)$ takes to drop from the peak to zero becomes long. In Figure 5(b), $M(t)$ increases from 4 to 34 as b_k varies from 0.10 to 0.135. The corresponding reliability function is shown in Figure 5(c). The curve becomes flat as the parameter b_k increases, which means that the reliability of the system is enhanced. These results indicate that as b_k increases, it becomes difficult for a trajectory to pass through the boundary and reach the target region B1.

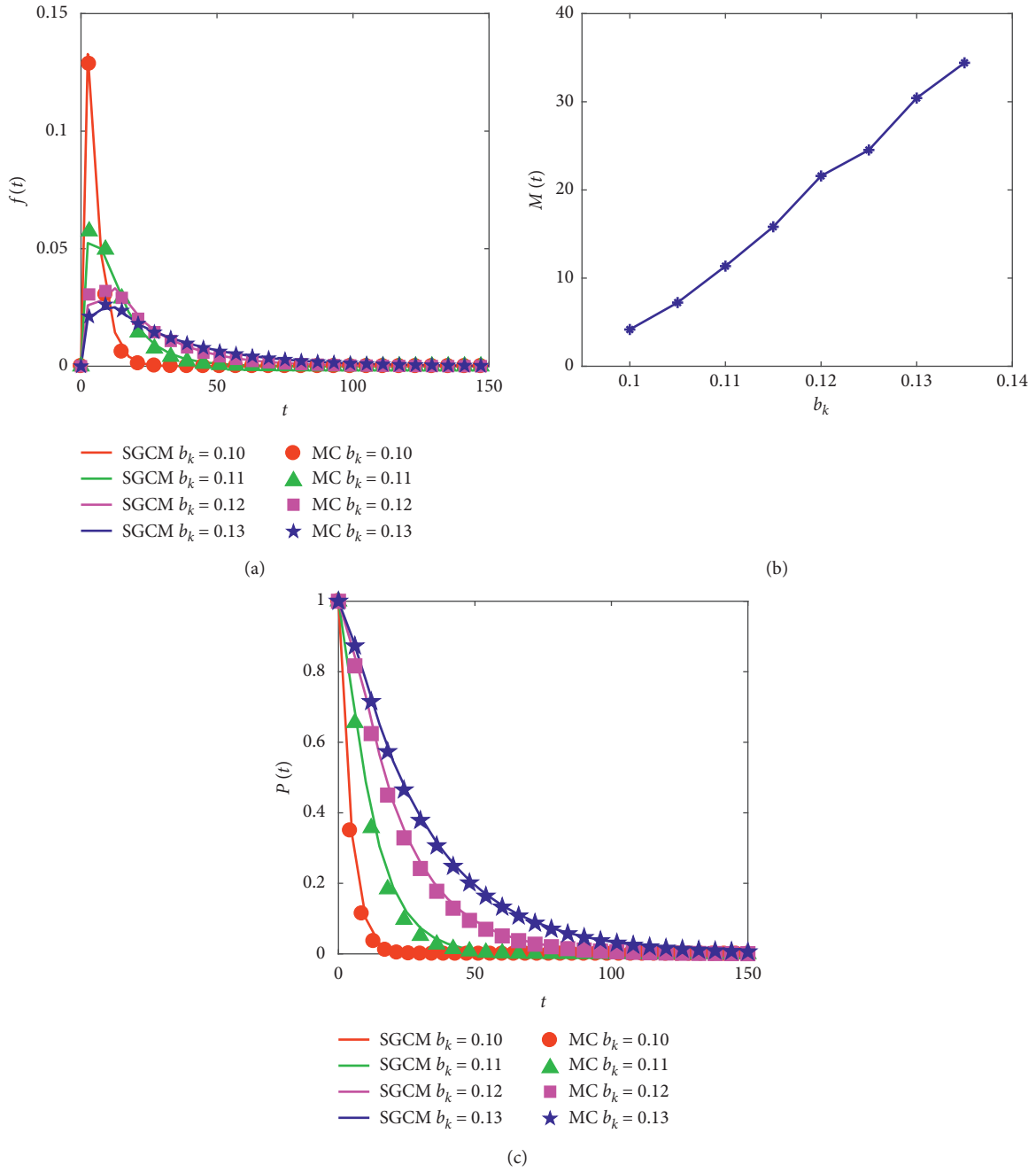

FIGURE 5: (a) Probability density function of FPT of system (6): $D = 0.20$, $\lambda = 0.20$. (b) MFPT of system (6): $D = 0.20$, $\lambda = 0.20$. (c) Reliability function of system (6): $D = 0.20$, $\lambda = 0.20$.

That is, the state transition in *B. subtilis* becomes difficult, which is consistent with the above phenomenon in Figure 4.

Next, the effect of parameter b_s is explored. Figure 6 shows the global dynamical character of system (5) for different b_s. As the b_s increases, the area of security domain B2 becomes large and the area of the target region B1 becomes small. This phenomenon theoretically indicates that the state transition becomes difficult.

Figure 7(a) shows the change of the PDF of FPT. As b_s increases, the peak of $f(t)$ gradually reduces, and the time that $f(t)$ takes to drop from the peak to zero becomes long. In Figure 7(b), $M(t)$ increases from 11 to 26 as b_s varies from 0.68 to 0.725. The corresponding reliability function is shown in Figure 7(c). The curvature of curve decreases as b_s increases, which indicates that the reliability of the system is enhanced. Thus, with the increase of b_s, it becomes difficult for a trajectory to pass through the boundary and reach the target region B1, which means the state transition in *B. subtilis* becomes difficult. The conclusion is in accordance with the above phenomenon in Figure 6.

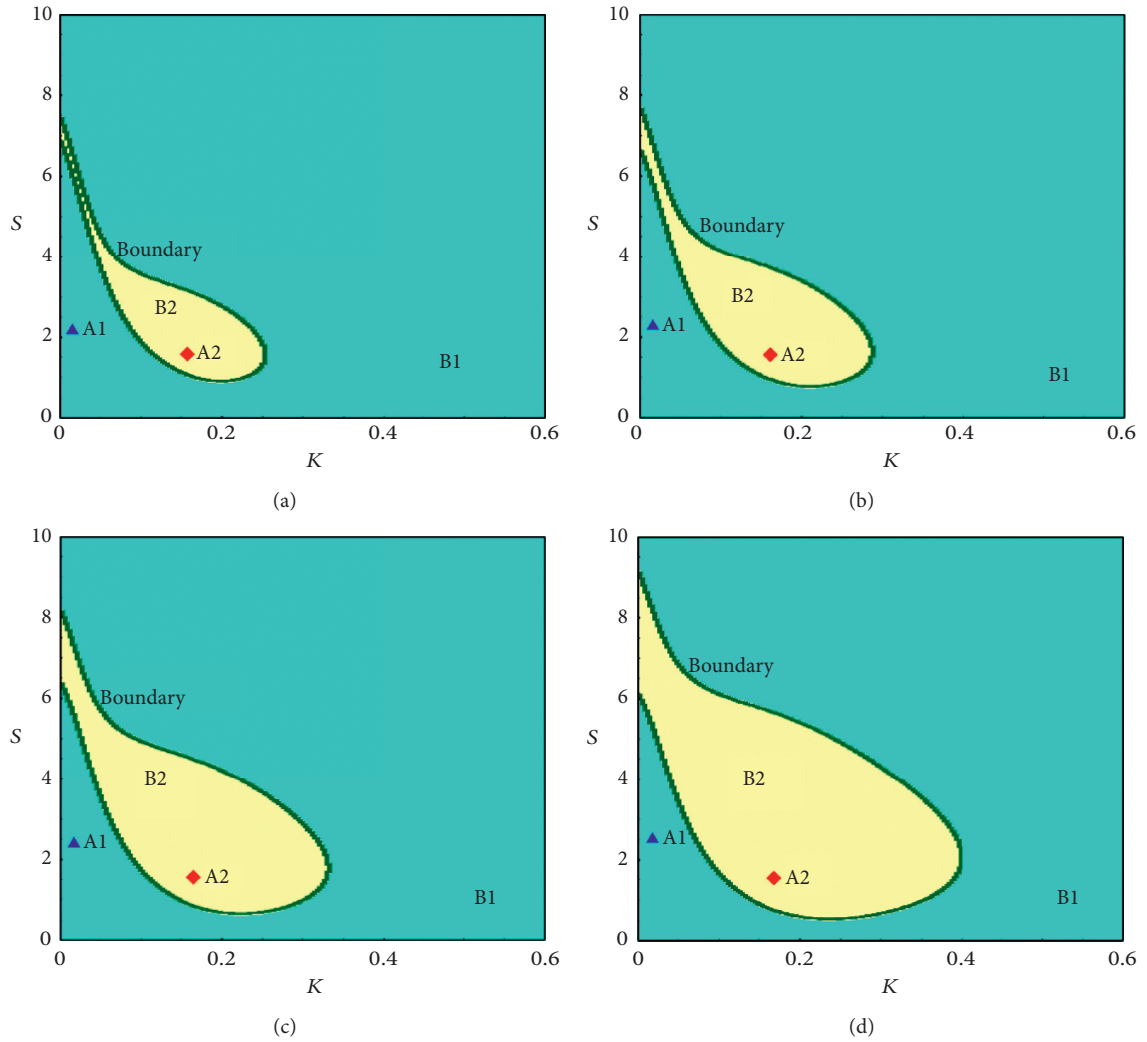

Figure 6: The global dynamic character of system (4): $b_k = 0.14$, (a) $b_s = 0.68$, (b) $b_s = 0.69$, (c) $b_s = 0.70$, and (d) $b_s = 0.71$.

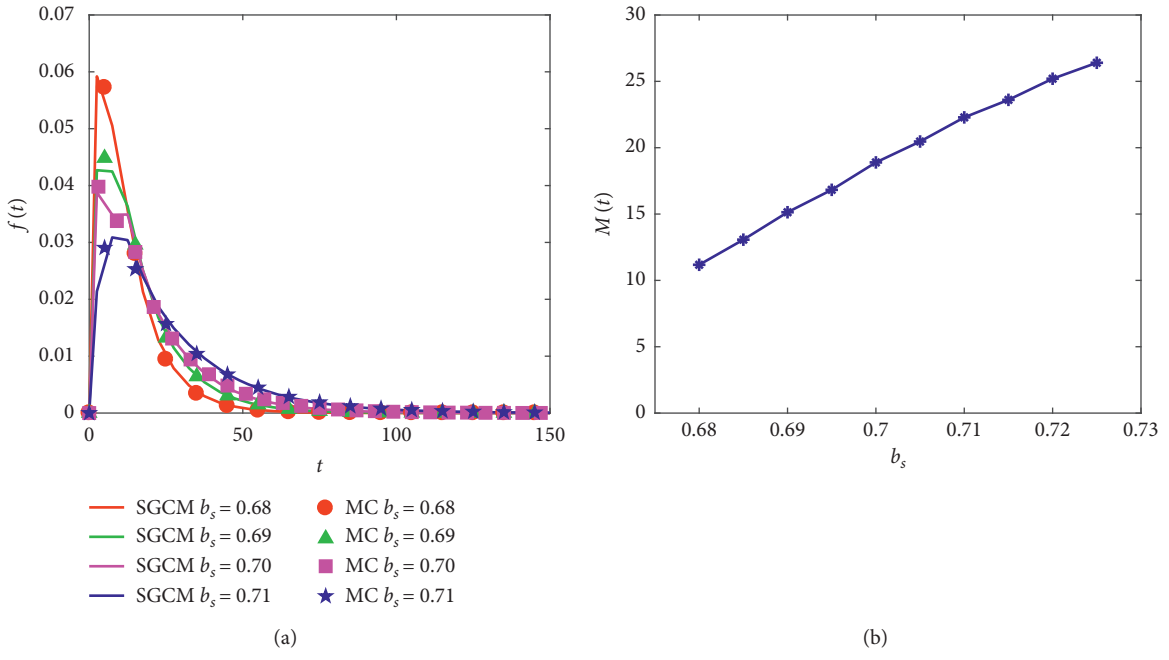

Figure 7: Continued.

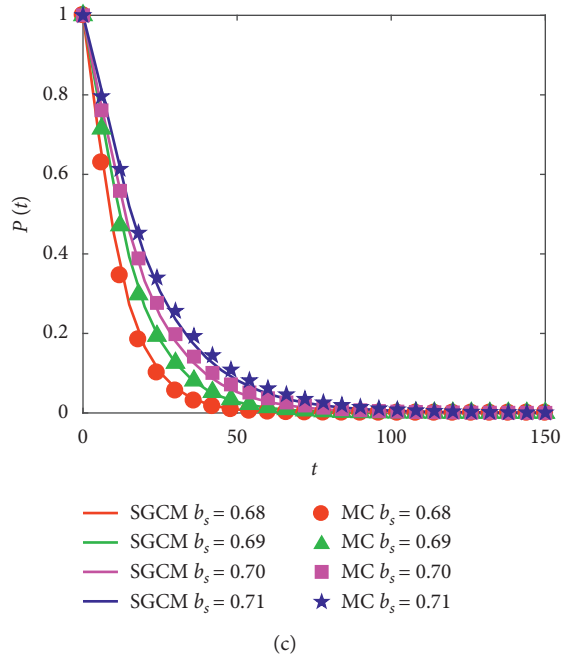

(c)

Figure 7: (a) Probability density function of FPT of system (6): $D = 0.20$, $\lambda = 0.20$. (b) MFPT of system (6): $D = 0.20$, $\lambda = 0.20$. (c) Reliability function of system (6): $D = 0.20$, $\lambda = 0.20$.

5. Conclusions

In this paper, we focus on the time of transition from competent state to vegetative state in *B. subtilis*. Thus, the stochastic exit problem of the gene regulatory circuit in *B. subtilis* affected by the colored noise is investigated through the three quantities related to the time: the PDF of FPT, MFPT, and the reliability function.

The results show that noise parameters and system parameters have significant effect on the state transition (from competent to vegetative state). As noise parameter D or λ increases, the state transition in *B. subtilis* becomes easy and the reliability of the system is weakened. Conversely, with the increase of system parameters b_k or b_s, the state transition in *B. subtilis* becomes difficult and the reliability of the system is enhanced. In addition, the effectiveness of the SGCM method is verified by MC simulation.

Data Availability

No data were used to support this study.

Conflicts of Interest

The authors declare that there are no conflicts of interest regarding the publication of this paper.

Authors' Contributions

The study was carried out in collaboration among all authors. All authors read and approved the final manuscript.

Acknowledgments

This research was supported by National Natural Science Foundation of China (Grant nos.11972289, 11672230, 11672231, and 11672232), Natural Science Basic Research Plan in Shaanxi Province (Grant no. 2018JM1043), and the Central University Fundamental Research Fund (Grant no. 3102018ZY043).

References

[1] A. Koseska, E. Ullner, E. Volkov, J. Kurths, and J. García-Ojalvo, "Cooperative differentiation through clustering in multicellular populations," *Journal of Theoretical Biology*, vol. 263, no. 2, pp. 189–202, 2010.

[2] G. M. Süel, J. Garcia-Ojalvo, L. M. Liberman, and M. B. Elowitz, "An excitable gene regulatory circuit induces transient cellular differentiation," *Nature*, vol. 440, no. 7083, pp. 545–550, 2006.

[3] N. Nandagopal and M. B. Elowitz, "Synthetic biology: integrated gene circuits," *Science*, vol. 333, no. 6047, pp. 1244–1248, 2011.

[4] N. Rosenfeld, J. Young, U. Alon, P. Swain, and M. Elowitz, "Gene regulation at the single-cell level," *Science*, vol. 307, no. 5717, pp. 1962–1965, 2005.

[5] D. Schultz, E. Ben Jacob, J. N. Onuchic, and P. G. Wolynes, "Molecular level stochastic model for competence cycles in Bacillus subtilis," *Proceedings of the National Academy of Sciences*, vol. 104, no. 45, pp. 17582–17587, 2007.

[6] V. Kohar and M. Lu, "Role of noise and parametric variation in the dynamics of gene regulatory circuits," *NPJ Systems Biology and Applications*, vol. 4, no. 1, p. 40, 2018.

[7] S. H. Dandach and M. Khammash, "Analysis of stochastic strategies in bacterial competence: a master equation

approach," *PLoS Computational Biology*, vol. 6, no. 11, Article ID e1000985, 2010.

[8] R. L. Honeycutt, "Stochastic Runge-Kutta algorithms. II. colored noise," *Physical Review A*, vol. 45, no. 2, pp. 604–610, 1992.

[9] S. Douwe and G. Venema, "ComK acts as an autoregulatory control switch in the signal transduction route to competence in Bacillus subtilis," *Journal of Bacteriology*, vol. 176, no. 18, pp. 5762–5770, 1994.

[10] W. Q. Zhu and Y. J. Wu, "First-passage time of duffing oscillator under combined harmonic and white-noise excitations," *Nonlinear Dynamics*, vol. 32, no. 3, pp. 291–305, 2003.

[11] W. Li, W. Xu, J. Zhao, and Y. Jin, "First-passage problem for strong nonlinear stochastic dynamical systems," *Chaos, Solitons & Fractals*, vol. 28, no. 2, pp. 414–421, 2006.

[12] C. S. Hsu, "A theory of cell-to-cell mapping dynamical systems," *Journal of Applied Mechanics*, vol. 47, no. 4, pp. 931–939, 1980.

[13] X. Yue, W. Xu, and Y. Zhang, "Global bifurcation analysis of Rayleigh-Duffing oscillator through the composite cell coordinate system method," *Nonlinear Dynamics*, vol. 69, no. 1-2, pp. 437–457, 2011.

[14] L. Wang, M. Huang, W. Xu, and L. Jin, "The suppression of random parameter on the boundary crisis of the smooth and discontinuous oscillator system," *Nonlinear Dynamics*, vol. 92, no. 3, pp. 1147–1156, 2018.

[15] L. Wang, L. Xue, C. Sun, X. Yue, and W. Xu, "The response analysis of fractional-order stochastic system via generalized cell mapping method," *Chaos: An Interdisciplinary Journal of Nonlinear Scienc*, vol. 28, no. 1, Article ID 013118, 2018.

[16] L. Wang, M. Huang, X. Yue, W. Jia, and W. Xu, "The stochastic dynamical behaviors of the gene regulatory circuit in Bacillus subtilis," *AIP Advances*, vol. 8, no. 6, Article ID 065302, 2018.

[17] J. H. Yang, M. A. F. Sanjuán, H. G. Liu, G. Litak, and X. Li, "Stochastic P-bifurcation and stochastic resonance in a noisy bistable fractional-order system," *Communications in Nonlinear Science and Numerical Simulation*, vol. 41, pp. 104–117, 2016.

[18] J. Yang, M. Sanjuán, P. Chen, and H. Liu, "Stochastic resonance in overdamped systems with fractional power nonlinearity," *The European Physical Journal Plus*, vol. 132, no. 10, p. 432, 2017.

[19] L. Chen, J. Qian, H. Zhu, and J.-Q. Sun, "The closed-form stationary probability distribution of the stochastically excited vibro-impact oscillators," *Journal of Sound and Vibration*, vol. 439, pp. 260–270, 2019.

[20] A. D. Grossman, "Genetic networks controlling the initiation of sporulation and the development of genetic competence in Bacillus subtilis," *Annual Review of Genetics*, vol. 29, no. 1, pp. 477–508, 1995.

[21] L. W. Hamoen, G. Venema, and O. Kuipers, "Controlling competence in Bacillus subtilis: shared use of regulators," *Microbiology*, vol. 149, no. 1, pp. 9–17, 2003.

[22] C. V. Rao and A. P. Arkin, "Stochastic chemical kinetics and the quasi-steady-state assumption: application to the gillespie algorithm," *The Journal of Chemical Physics*, vol. 118, no. 11, pp. 4999–5010, 2003.